Methods

Nikola Fischer* and Franziska Mathis-Ullrich

Compact flexible actuator based on a shape memory alloy for shaping surgical instruments

Kompakt-flexible Aktuatoren aus Formgedächtnislegierung zur Formgebung chirurgischer Instrumente

https://doi.org/10.1515/auto-2023-0049
Received March 31, 2023; accepted May 31, 2023

Abstract: Conventional flexible actuators for minimally invasive interventions come with complex and bulky actuation infrastructure. We present a proof-of-concept study of a compact flexible actuator with variable shape change featuring shape memory alloy wire loops in active-antagonist configurations for a bending and S-shape. The actuator was fabricated using heat-treated wire loops. The evaluation using optical marker tracking revealed a mean maximum absolute displacement at the distal tip of 19 mm and a force of 90 mN reached in under 15 s. For control, a closed-loop regime was evaluated with steady-state errors below 2°.

Keywords: flexible instrument; minimally invasive surgery; shape memory alloy

Kurzfassung: Flexible Aktuatoren für minimalinvasive Eingriffe benötigen häufig eine umfangreiche Infrastruktur zur Energieübertragung. Wir demonstrieren das Konzept eines kompakten, variablen Aktuators mit kontrollierbarer Formänderung. Er besteht aus zwei wärmebehandelten Drahtschleifen aus Formgedächtnislegierung in einer antagonistischen Konfiguration für eine reine Biegung und eine S-Form. Die Untersuchung der Formänderung mittels optischem Marker Tracking ergab eine mittlere maximale Auslenkung an der distalen Spitze von 19 mm und eine Kraft von 90 mN in weniger als 15 s. Im geschlossenen Regelkreis wurden stets stationäre Abweichungen unter 2° ermittelt.

Schlagwörter: Formgedächtnislegierung; Flexible Instrumente; Minimalinvasive Chirurgie

***Corresponding author: Nikola Fischer**, Institute for Anthropomatics and Robotics (IAR), Karlsruhe Institute of Technology (KIT), 76131 Karlsruhe, Germany, E-mail: nikola.fischer@kit.edu. https://orcid.org/0000-0001-9364-3328
Franziska Mathis-Ullrich, Department Artificial Intelligence in Biomedical Engineering (AIBE), Friedrich-Alexander University Erlangen-Nürnberg (FAU), 91052 Erlangen, Germany

1 Introduction

1.1 Motivation

Non-invasive and minimally invasive surgery (MIS) present themselves as promising alternatives compared to conventional open surgery due to a lower infection risk and shorter time spent post-op in a medical facility [1]. These advantages are achieved by using special instruments during surgery that can be inserted into the body of the patient through either natural orifices (e.g., mouth, anus) or a limited amount of small incisions. Such instruments have the purpose to provide visual imaging to the medical experts and let them dexterously perform surgical actions such as cutting and grasping within the body cavities. Simple flexible actuators and sophisticated continuum robots can both extend the user's scope and operation space even in difficult-to-access operation sites. That includes the navigation within the human body, e.g., inside the winding organs of the gastrointestinal tract, as well as in neurosurgery, where critical structures must be avoided by using more complex paths around them [2].

Common actuation methods of continuum robots include pneumatic, hydraulic, electromagnetic, and tendon drives [3]. Continuum robots are numerically controllable manipulators with an infinite number of joints [4] and can be customized to adapt to a specific task. Their design and control remains challenging due to their hyper-redundant characteristic [5] where the number of degrees-of-freedoms (DOFs) exceeds the number of individually controllable actuators. Facing this challenge, aforementioned approaches afford bulky setups such as fluid pumps and valves for pneumatic and hydraulic systems or multiple electric motors for tendon pulling. Consequently, a desired scaling of the robotic structure toward smaller diameters, greater lengths, and larger bending angles is limited. Thus, for usage of controllable and flexible instruments in MIS these aspects of design and performance remain key.

Smart materials such as shape memory alloys (SMA) seem promising when facing those challenges due to their ability to *memorize* an almost arbitrary shape when traversing a reversible crystal phase change from martensite to austenite caused by increasing temperature, referred to as the *shape memory effect*. If a task requires one particular target pose including a specific shape of the robotic structure, the SMA actuators can be prepared accordingly in advance (shape setting) and reach that shape in a controlled manner during the actual task execution using simple electric power circuits with little space demand. SMA in the form of wires can provide a higher power-to-weight-ratio than conventional electric motors, they are simpler to implement than other smart materials such as electroactive polymers (EAPs) and allow for larger displacements than piezoceramics [6]. SMA wires are deployed within actuators as quasi-elastic components or as dampers [7] due to their superelastic strain. Furthermore, they can provide linear motion, making use of the SMA for repeatable (workable) strains of up to 5 % [8] when heated via conduction or via Joule heating. Moreover, the linear relation between electric resistance and strain enables SMA actuators' self-sensing-potential for dual-use as an actuator that is able to sense its position and even further ambient parameters [9]. Therefore, SMAs show great potential for simplified, integrated, scalable and customized actuation of various robotic applications.

1.2 Related work

A widely used actuation principle for continuum robots is the tendon drive, where tendons are pulled by at least one rotatory [10] or linear motor [11] per DOF for each segment, eventually leading to bulky and complex hardware setups. To minimize space requirements, tendons could be replaced by SMA wires or spring coils, which create pulling forces by contraction. Despite the aforementioned large strains, SMA wires must come at great lengths to achieve sufficient bending. Besides those physical bending angle constraints, electronic connectors are required on each end of every SMA actuator [12], leading to a complex, error-prone electronic setup with increased initial load, which is additionally hard to integrate into a delicate device. To compensate for the bending constraint, Allen and Swensen [13] propose a hybrid of SMA and pneumatic actuation, reaching bending angles >180° at the cost of an additional setup for air pressure supply. In Ref. [14], SMA wires are deployed as 'free-sliding' tendons within a polymeric substrate and allow for bending angles of up to 400°. When combining multiple of such segments in a serial configuration by rigid links, a hyper-redundant robotic structure occurs, where multiple DOFs can be actuated independently allowing for various complex robotic shapes promising high dexterity and precise controlling of every segment pose [5]. When it comes to the interconnection between those segments, SMAs could be deployed in a straight manner [15], within a pulley system, and in a purely antagonistic configuration, with an elastic joint or a hybrid combination [16]. When including the SMA's self-sensing ability, even closed-loop control regimes can be realized [17], e.g., for 3D-manipulation of a needle tip in real-time. For further sensing modalities, Ren et al. [18] present a flat soft actuator from elastomer for variable stiffness applications, including embedded SMA and curvature sensors.

1.3 Contribution

The immediate utilization of the *shape memory effect* has the potential to overcome several existing challenges, such as extending the bending range by creating a suitable shape memory independent of excessive longitudinal strains, to reduce space requirements compared to conventional actuation approaches with large external manipulation and simplifying the electric actuation setup drastically. In this work, we aim to investigate this potential by deploying two SMA wire loops with electrical contacts in proximity and with different shape memories alongside each other. Thus, we provide a proof-of-concept of a novel, shape changing actuator that is able to perform controlled bending and straightening motion for dexterous tasks during MIS.

2 Materials and methods

The investigation includes the design, fabrication, control and experimental evaluation of the novel flexible actuator unit in two different shape configurations.

2.1 Design

The novel actuator consists of two SMA wire loops from nickel-titanium-copper (NiTiCu) forming a skeleton that provides individual actuation once heated above their austenite finish temperature A_f = 65 °C. They are embedded in a monolithic flexible backbone and surround a central supply channel that connects proximal and distal ends of the actuator. The channel provides space for instruments such as fiber optics or bendable needles. The actuator's proximal end allows for insertion of instruments and to attach the contact electrodes for (controlled) power supply. Several spacer discs serve as wire guidance along the actuator to avoid short circuits. No further cable connection is required for power or control actuation. For this work, two different instrument configurations were investigated and fabricated, as illustrated in Figure 1. Configuration (I) for a bending and (II) for an S-shape of the actuator. Both shape changes are independently obtained by an active-antagonist configuration, as described in Ref. [16]. Thus, each configuration features one SMA wire loop *memorizing* a shape change

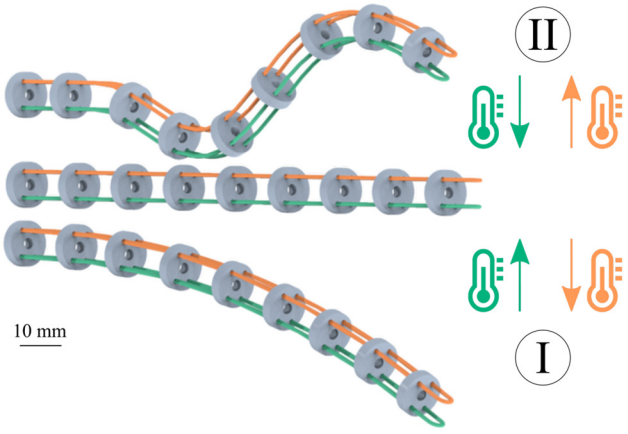

Figure 1: Concept of the compact flexible actuator for minimally invasive instruments featuring two shape memory alloy (SMA) wire loops with preset shape memory for shape changing (orange), reset into straight shape (green) and central supply channel, e.g., for a gripping tool. The desired shapes are bending (I) and S-shape (II).

(bending or S-shape, respectively) referred to as *shape loop* (active). The other loop sets back the actuator to its initial straight shape, referred to as *straight loop* (antagonist). This design allows for a permanently retained pose of the distal tip without further heating if no external force is applied.

2.2 Fabrication and assembly

Fabrication steps are presented in Figure 2. In step 1, segments of SMA wire with a diameter of 0.7 mm are cut with a length of 230 mm and cold-formed manually into a U-shape (loop) with a diameter of 3 mm. To set the shape memory in step 2 for straight shape, bent shape and S-shape, heat treatment at 425 °C for 30 min and subsequent quenching in water at room temperature is required for the loop segments [19, 20]. Thereby, each loop segment must be clamped firmly in the desired shape and without torsion stress as it tries to restore its previous shape memory, i.e., the straight shape. Thus, holding racks are fabricated from aluminum, providing the desired curvature of the shapes to stabilize the loop segments during heat treatment. After heat treatment, all wire loops are cold-formed into straight shape at room temperature in step 3. In step 4, the flexible monolithic backbone with intermediate spacer disks and central supply channel is 3D-printed using a stereolithography printer with elastic resin (Formlabs GmbH, Germany). To allow for accurate evaluation, the flexible backbone model is extended for a mounting component at the proximal end and plane elements at each spacer disk for marker attachment. The wire loops are inserted into the printed backbone before its final curing. Thus, the fully cured backbone holds the SMA wires firmly throughout actuation.

3 Experimental evaluation

3.1 Actuation setup

The actuator is mounted at its proximal end in a horizontal position and connected to a laboratory power supply. Once electrified, joule heating increases the temperature of the SMA wires, resulting in the wires memorizing their shape leading to an active shape change, and an antagonistic reset, respectively.

3.2 Visual tracking and actuator shape

To control and characterize the flexible actuator, shape estimation of its body is required. For visual tracking, a

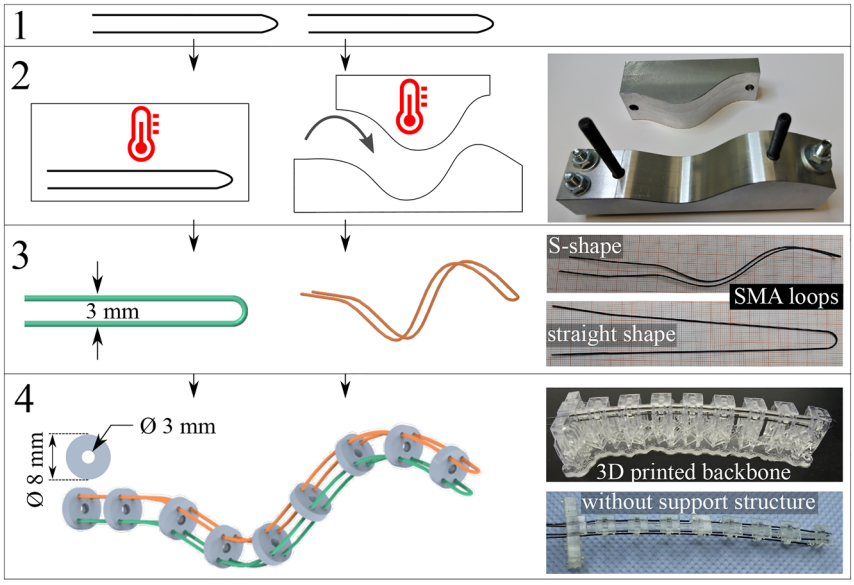

Figure 2: Fabrication steps. Cold-forming wire loops (1), followed by heat treatment with customized aluminum racks at 425 °C (2). All wire loops are straightened by cold-forming (3) and inserted in the 3D printed monolithic backbone, followed by the final curing of the actuator (4).

RealSense™ D435 camera (Intel Corporation, USA) observes the x-y-plane, tracking nine ArUco-markers attached to the actuator body, as presented in Figure 4a and c. A tracking algorithm is implemented in Python and provides a tracking frequency of 30 Hz. Thus, the positions of the geometrical marker center points provide time-depending shape information. Its performance was evaluated beforehand by tracking a stationary set of markers as utilized on the actuator over a time period of 90 s, revealing a deviation of ± 0.35 mm and ± 0.05 mm in x and y, respectively. The pose for configuration I is represented by the distal end's bending. For simplicity, the two markers closest to the distal tip are used to define the actuator's orientation as the angle φ relative to the x-axis.

3.3 Control

To manipulate the flexible actuator, a PID-controller is proposed in a closed-loop regime as shown in Figure 3 with the iteratively identified control parameters $K_P = 50$, $K_I = 0.5$ and $K_D = 0.8$. The control variable is the bending angle φ of the distal tip. Further shape modeling parameters are currently not considered. For implementation, an ATmega328 (Arduino) microcontroller is deployed using two DC/DC-converters TSR-3 Series (Traco Electronic GmbH, Germany) that can perform each 3 A switching regulation via remote on/off input connected to the pulse-width-modulation (PWM) outputs of the microcontroller at 10 Hz. The computed angle φ is transmitted from the Python script to the microcontroller via Serial Port.

3.4 Evaluation methods

Each configuration passes $n = 10$ experiment runs for workspace characterization, with 180 s cooling pauses in between. For configuration I, we additionally conducted a control evaluation and a qualitative force validation. To characterize the full workspace of the actuator, the shape loop is initially heated at current $I = 3$A ($U_{\max} = 2.6$ V) from initial straight shape and the displacement of all markers is monitored over 15 s. A (passive) cooling period of 30 s follows, during which the power supply is switched off. Then, the straight loop is heated for another 15 s. After a second cooling period of 30 s, the experiment is stopped. The cooling periods allow for investigation of possible recoils in scenarios without power supply. Before the next experiment run starts, the actuator is manually cold-formed to its initial straight shape. For force measurement, a spring scale (Micro-Line 20001 1 N, Pesola AG, Switzerland) is insulated at its interface and attached to the distal tip of the actuator (configuration I). Then, $I = 3$A is applied, and the resulting force is measured. The control regime is demonstrated by following predefined setpoints from straight to bending shape, i.e., φ_{ref} from 0° to 10° in iteration steps of 2°, each lasting for 15 s.

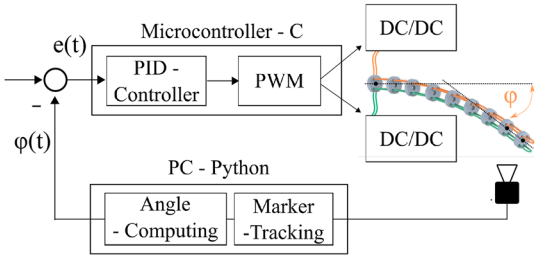

Figure 3: Closed-loop control setup including marker tracking, angle computation using a Python script and a PID-Controller running on a microcontroller.

4 Results

Figure 4b presents the mean marker positions and standard deviations at given times of the proposed actuator in configuration I. The maximum absolute displacement is 19.1 mm in y at the distal tip. During the cooling period, a recoil is visible, retaining an absolute displacement of the distal tip at $y < 12$ mm between $t = 15$ and 45 s. Heating the straight loop, in order to return the actuator to its initial shape, leaves the actuator with a remaining absolute displacement of $y > 5$ mm. Thereafter, another small recoil can be observed between $t = 60$ and 90 s.

Figure 4c shows configuration II in an actuated state. The planar S-shape exhibits an unintended torsion, visible on the basis of the last three markers at the distal tip. We assume that the SMA wire was slightly axially rotated at the distal part during assembly with the backbone, despite utmost caution. This would lead to a deviation from the strict planar shape change, and unintentionally demonstrating that our approach is not limited to planar shapes.

Figure 4d shows the workspace characterization results for configuration II. A maximum displacement of $y = 8.7$ mm is observed close to the distal tip at $t = 60$ s. The antagonistic setback of the proximal actuator half is noticeable, while the distal half does not exhibit a significant shape deformation back to the straight shape. Presumably, the aforementioned torsion influenced the plane of bending for the distal actuator half, leading to an apparently restrictive setback in the x-y-plane.

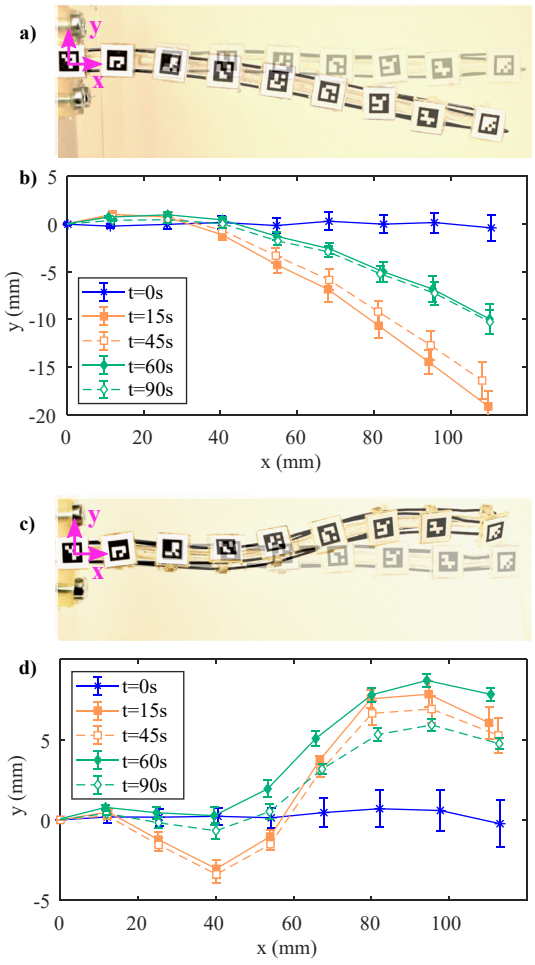

Figure 4: Results of the workspace characterization for configuration I and II, showing initial pose (translucent) and maximum deflection (a and c). Estimated shape using mean and standard deviation of marker positions at specific time steps over $n = 10$ experiment runs (b and d). The obtained shape change (orange) is reversed by the subsequent straightening (green). Dashed plots indicate the observed recoils after actuation has ended.

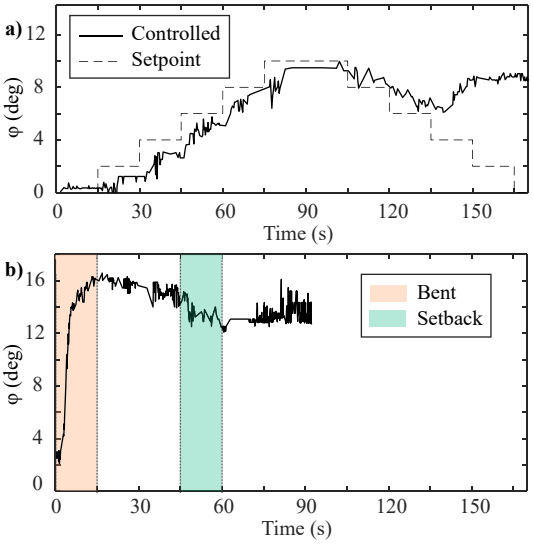

Figure 5: Bending angle φ for configuration I controlled in closed-loop for setpoints φ_{ref} (a). In contrast, bending angle φ for configuration I during characterization, with actuation phases for bending (orange) and setback (green) in open-loop control (b).

Furthermore, stronger recoils are measured as with configuration I. It should be noted that deflections in the initial poses ($t = 0$ s) are caused by manual resetting the actuator after each experiment run.

In Figure 5a, the results of closed loop control of the actuator are presented. A steady-state error of $\varphi_{error} < 2°$ is observed for larger setpoints. After reaching the maximum setpoint (at 10°), angle control is lost at approximately $\varphi = 9°$.

Figure 5b depicts an actuation with open-loop control for comparison, visualizing a much steeper bending characteristic and reaching a maximum bending angle within 15 s.

Furthermore, the force measurement revealed a maximum force applied by the distal tip of 90 mN.

5 Discussion

The workspace characterization reveals a repeatable deformation for both configurations. Although the deviation range appears usable for a handheld device, normally exposed to physiological tremor of the user, one single target shape presents an essential limitation in comparison with omnidirectional bending actuators, such as in Ref. [12].

In contrast, our approach does not require multiple individually supplied and actuated sections to transform into more complex shapes (e.g., S-shape), allowing for a smaller instrument diameter and a more compact actuation unit. For example, neglecting power supply (socket or battery) and microcontroller (which are required for all presented systems), the actuator only requires one DC/DC converter with a frame package size of $<1\,cm^3$ and two wire channels for one wire loop per desired shape. Yet in direct comparison to [12], the maximal workspace of our demonstrator is smaller, the antagonistic setback capability more restricted (especially for S-shape), and the response time slower, presumably due to the deployment of two SMA wire loops that reinforce and stiffen the flexible structure, thereby hindering the active wire loop mechanically, even

when not actuated. This might be also the cause for the observed recoil. Furthermore, the method of passive cooling and the length of the cooling time in this work may not be optimal. Thus, a higher temperature in the shape loop could keep it from becoming fully inactive during the antagonistic setback. We will investigate this hypothesis by including temperature monitoring in future experimental setups.

On the other hand, the increased stiffness of our actuator brings the advantage to avoid unintended displacement and deformation during insertion of additional instruments through the central supply channel (e.g., fiber endoscopes).

Regarding angle control, a notable path correction can be observed when comparing the angles obtained during closed-loop and open-loop control. A small error of the bending angle for the increasing setpoint values demonstrates the effect of closed-loop SMA actuation. However, the loss of control after a longer period of actuation shows one major challenge of SMA-based robotics. When heating the actuator wire loops over a longer period of time, they no longer leave the austenite phase but remain above the transformation temperature of 60 °C. Thus, the actuator stiffens and remains at its current position, where additional heating has little effect on the shape. Only a temperature change below the transformation temperature, unlocks the actuator. Hence, active cooling strategies should be considered for *in-vivo* use cases where multiple setpoints are targeted over a short period of time, causing heat accumulation.

The transition temperature of the currently used material does not appear eligible for a surgical instrument yet, as it could damage the human tissue. Alloy compositions with transition temperatures of ≈ 40 °C are more promising for future investigations into instrument design and fabrication.

The maximum applicable force is measured to be relatively small but still in a relevant range for applications in ophthalmology (retraction, penetration) and vascular surgery (vascular clamping) [21].

6 Conclusions

Our results demonstrate that multiple SMA wire loops can be combined in one actuator to create various bending motions and setbacks toward their initial pose with minimal space demand. Thus, the presented actuator proof-of-concept shows the potential as a space-effective alternative to shape a handheld surgical instrument, immediately utilizing the shape memory effect of SMA materials, for a certain target shape required to address known navigation challenges.

However, the disadvantages of a limited workspace and the potential loss of control due to overheating may jeopardize the benefit of the actuator in the clinical environment. Therefore, it is crucial to identify those surgical procedures that can benefit even from small, anticipated shape changes and small applicable forces within a limited time window.

Future research shall address 3D-shape changes and design optimization regarding workspace enlargement, improved temperature management, and the deployment of the self-sensing ability of SMA materials to make visual tracking obsolete.

Acknowledgment: The authors would like to thank Heiko Engelhardt and Monsur Islam for their support on material procurement and heat treatment.
Author contributions: All the authors have accepted responsibility for the entire content of this submitted manuscript and approved submission.
Research funding: None declared.
Conflict of interest statement: The authors declare no conflicts of interest regarding this article.

References

[1] K. Imaizumi, S. Homma, Y. Miyaoka, et al., "Exploration of the advantages of minimally invasive surgery for clinical T4 colorectal cancer compared with open surgery: a matched-pair analysis," *Medicine*, vol. 101, no. 32, p. e29869, 2022.
[2] S. Peikert, C. Kunz, N. Fischer, et al., "Automated linear and non-linear path planning for neurosurgical interventions," in *2022 International Conference on Robotics and Automation (ICRA)*, 2022, pp. 7731—7737.
[3] J. Burgner-Kahrs, D. C. Rucker, and H. Choset, "Continuum robots for medical applications: a survey," *IEEE Trans. Robot.*, vol. 31, no. 6, pp. 1261—1280, 2015.
[4] B. Siciliano and O. Khatib, *Springer Handbook of Robotics*, Cham, Springer, 2016.
[5] G. S. Chirikjian and J. W. Burdick, "A hyper-redundant manipulator," *IEEE Robot. Autom. Mag.*, vol. 1, pp. 22—29, 1994.
[6] V. D. Sars, S. Haliyo, and J. Szewczyk, "A practical approach to the design and control of active endoscopes," *Mechatronics*, vol. 20, no. 2, pp. 251—264, 2010.
[7] S. Kumar, P. Shivashankar, and S. Gopalakrishnan, "A half a decade timeline of shape memory alloys in modeling and applications," *ISSS J. Micro Smart Syst.*, vol. 9, no. 1, pp. 1—32, 2020.
[8] Z. Shang, J. Ma, Z. You, and S. Wang, "A braided skeleton surgical manipulator with tunable diameter," in *2020 8th IEEE RAS/EMBS International Conference for Biomedical Robotics and Biomechatronics (BioRob)*, 2020, pp. 223—228.
[9] S. J. Furst, J. H. Crews, and S. Seelecke, "Stress, strain, and resistance behavior of two opposing shape memory alloy actuator wires for resistance-based self-sensing applications," *J. Intell. Mater. Syst. Struct.*, vol. 24, no. 16, pp. 1951—1968, 2013.

[10] B. Ouyang, Y. Liu, and D. Sun, "Design of a three-segment continuum robot for minimally invasive surgery," *Robot. Biomimetics*, vol. 3, no. 1, p. 2, 2016.
[11] G. Palli and S. Pirozzi, "A miniaturized optical force sensor for tendon-driven mechatronic systems: design and experimental evaluation," *Mechatronics*, vol. 22, no. 8, pp. 1097—1111, 2012.
[12] M. R. A. Kadir, D. E. O. Dewi, M. N. Jamaludin, M. Nafea, and M. S. M. Ali, "A multi-segmented shape memory alloy-based actuator system for endoscopic applications," *Sens. Actuators A*, vol. 296, pp. 92—100, 2019.
[13] E. Allen and J. Swensen, "Design of a highly-maneuverable pneumatic soft actuator driven by intrinsic SMA coils (PneuSMA actuator)," in *IEEE/RSJ International Conference on Intelligent Robots and Systems (IROS)*, 2020, pp. 8667—8672.
[14] J. H. Lee, Y. S. Chung, and H. Rodrigue, "Long shape memory alloy tendon-based soft robotic actuators and implementation as a soft gripper," *Sci. Rep.*, vol. 9, no. 1, p. 11251, 2019.
[15] W. Wang, Y. Tang, and C. Li, "Controlling bending deformation of a shape memory alloy-based soft planar gripper to grip deformable objects," *Int. J. Mech. Sci.*, vol. 193, p. 106181, 2021.
[16] D. Reynaerts, J. Peirs, and H. Van Brussel, "Shape memory micro-actuation for a gastro-intestinal intervention system," *Sens. Actuators A*, vol. 77, no. 2, pp. 157—166, 1999.
[17] B. Konh, P. Berkelman, and S. Karimi, "Needle tip manipulation and control of a 3d steerable sma-activated flexible needle," in *2020 8th IEEE RAS/EMBS International Conference for Biomedical Robotics and Biomechatronics (BioRob)*, 2020, pp. 903—909.
[18] Z. Ren, M. Zarepoor, X. Huang, A. P. Sabelhaus, and C. Majidi, "Shape memory alloy (SMA) actuator with embedded liquid metal curvature sensor for closed-loop control," *Front. Robot. AI*, vol. 8, pp. 1—12, 2021.
[19] C. Haberland and M. H. Elahinia, "Fabricating NiTi SMA components," in *Shape Memory Alloy Actuators: Design, Fabrication and Experimental Evaluation*, 2015, pp. 191—238.
[20] A. Rao, A. R. Srinivasa, and J. N. Reddy, "Manufacturing and post treatment of SMA components," in *Design of Shape Memory Alloy (SMA) Actuators*, vol. 3, Cham, Springer, 2015.
[21] A. K. Golahmadi, D. Z. Khan, G. P. Mylonas, and H. J. Marcus, "Tool-tissue forces in surgery: a systematic review," *Ann. Med. Surg.*, vol. 65, p. 102268, 2021.

Bionotes

Nikola Fischer
Institute for Anthropomatics and Robotics (IAR), Karlsruhe Institute of Technology (KIT), 76131 Karlsruhe, Germany
nikola.fischer@kit.edu
https://orcid.org/0000-0001-9364-3328

Nikola Fischer is a doctoral candidate and currently working as a researcher at the Karlsruhe Institute of Technology (KIT) at the department for Pervasive Computing Systems (TECO). Before joining KIT in 2020, he was a research assistant at the Hamlyn Centre for Robotic Surgery at Imperial College London. He received his B.Eng. in Mechanical Engineering at the University of Applied Sciences Karlsruhe (HKA) in 2017 and his M.Sc. in Mechatronic and Micro-Mechatronic Systems at HKA and École Nationale Supérieur de Mécanique et des Microtechniques in Besançon, France in 2019. His research focuses on the application of smart materials in the field of health robotics, especially for flexible instruments and continuum robots in minimally invasive surgery.

Franziska Mathis-Ullrich
Department Artificial Intelligence in Biomedical Engineering (AIBE), Friedrich-Alexander University Erlangen-Nürnberg (FAU), 91052 Erlangen, Germany

Franziska Mathis-Ullrich is professor for surgical robotics at the Friedrich-Alexander-University Erlangen-Nürnberg (FAU) at the Dep. Artificial Intelligence in Biomedical Engineering. Before joining FAU in 2023, she was assistant professor at the Karlsruhe Institute of Technology (KIT) since 2019. Her primary research focus is on minimally invasive and cognition controlled robotic systems and embedded machine learning with emphasis on applications in surgery. She received her B.Sc. and M.Sc. degrees in mechanical engineering and robotics in 2009 and 2012 and obtained her Ph.D. in 2017 in Microrobotics from ETH Zurich, respectively.